Annales Societatis Geologorum Poloniae (2023), vol. 93: 305–322 https://doi.org/10.14241/asgp.2023.10

FATE OF SWELLING CLAY MINERALS DURING EARLY DIAGENESIS: A CASE STUDY FROM GDAŃSK BAY (BALTIC SEA)

Marta KISIEL[1,*], Michał SKIBA[1], Mateusz DAMRAT[2], Artur KULIGIEWICZ[3], Katarzyna MAJ-SZELIGA[1], Magdalena MAKIEL[1], Marek ZAJĄCZKOWSKI[4], Dorota SALATA[1]

[1] *Jagiellonian University, Institute of Geological Sciences, Gronostajowa 3a, 30-387 Kraków, Poland; e-mails: m.kisiel@doctoral.uj.edu.pl, michal.skiba@uj.edu.pl, m.skoneczna@doctoral.uj.edu.pl, katarzyna.maj@uj.edu.pl, dorota.salata@uj.edu.pl*

[2] *Polish Geological Institute – National Research Institute, Rakowiecka 4, 00-975 Warsaw, Poland; e-mail: mateusz.damrat@pgi.gov.pl*

[3] *Institute of Geological Sciences, Polish Academy of Sciences, Senacka 1, 31-002 Kraków, Poland; e-mail: ndkuligi@cyf-kr.edu.pl*

[4] *Institute of Oceanology, Polish Academy of Sciences, Powstańców Warszawy 55, 81–712 Sopot, Poland; e-mail: trapper@iopan.pl*

** Corresponding author*

Kisiel, M., Skiba, M., Damrat, M., Kuligiewicz, A., Maj-Szeliga, K., Makiel, M., Zajączkowski, M. & Salata, D., 2023. Fate of swelling clay minerals during early diagenesis: a case study from Gdańsk Bay (Baltic Sea). *Annales Societatis Geologorum Poloniae*, 93: 305–322.

Abstract: The aim of the study was to recognize the early diagenetic transformations of clay minerals likely taking place in the brackish environment of Gdańsk Bay (Baltic Sea). The Vistula River loads and sediments of the Vistula delta front and prodelta were studied. The mineral compositions of the clay fractions were determined by X-ray diffractometry. The average layer charge (LC) of the expandable interlayers was determined using the O-D vibrational spectroscopy method. The major element content of the studied clays was determined by inductively coupled plasma optical emission spectrometry. The <0.2 μm clay fraction, separated from the river sediments, contained illite-smectite mixed layered minerals, rich in high-charge, dioctahedral smectite (Ilt-Sme), illite, and kaolinite. The same clay fraction, separated from the delta-front sediments, was also composed mainly of Ilt-Sme, illite, kaolinite, and hydroxy-interlayered minerals. The <0.2 μm clay fraction from the prodelta sediments was depleted in Ilt-Sme and enriched in illite and chlorite, relative to the clays from both the river and the delta-front sediments. The LCs (0.45 to 0.56 per formula unit) were higher for clays from the river and the delta front sediments, relative to the clays from the prodelta. The <0.2 μm clay fractions from the prodelta sediments were enriched in MgO, Fe_2O_3, and K_2O, relative to the fine clay fraction from the river. The results indicated that the smectite component of Ilt-Sme, deposited by the Vistula in Gdańsk Bay, underwent chloritization and likely illitization. The chloritization most likely proceeded via formation of hydroxy-interlayers within the smectite. Illite-like minerals, formed at the expense of the smectite with high LC, due to selective adsorption and fixation of K^+ from seawater.

Key words: Smectite, chlorite, illite, reverse weathering, brackish environment, contemporary sediments, O-D method.

Manuscript received 5 December 2022, accepted 28 March 2023

INTRODUCTION

Two major processes controlling clay composition in recent marine sediments are (1) inheritance of terrigenous clays via deposition of rivers loads and (2) early diagenetic formation of clay minerals, also known as reverse weathering. Chamley (1989) and Weaver (1989), each summarizing almost four decades of research into the clay mineralogy of sediments in deltas and estuaries, came to the general conclusion that land-derived aluminous swelling clays do not undergo any significant transformations during early diagenesis in marine environments and therefore the clay mineralogy of young marine sediments is controlled exclusively by detrital input. Although the distribution of phyllosilicates on

the ocean floor indeed reflects the products of the primary weathering regimes of specific climate zones (Griffin *et al.*, 1968; Chamley, 1989), which may indicate that terrigenous clay minerals do not undergo any changes within the marine environment, numerous studies show that once introduced into the ocean environment, terrigenous clay minerals are no longer stable (Michalopoulos and Aller, 1995; Hover *et al.*, 2002; Cuadros *et al.*, 2017; Isson and Planavsky, 2018).

Reverse weathering refers to the rapid neoformation of clay minerals and/or the transformation of land-derived clays in an ocean environment that take place during early diagenesis due to the consumption of dissolved cations from seawater. The process was introduced by Mackenzie and Garrels (1966), since then, it has been regarded as significant for controlling the chemical mass balance between rivers and oceans (Mackenzie and Kump, 1995; Michalopoulos and Aller, 1995; Isson and Planavsky, 2018; Isson *et al.*, 2020). Reverse weathering is believed to contribute to the low basicity of ocean water by releasing CO_2 and generating acidity. Therefore it constitutes an important component of the CO_2 cycle, which controls the chemical composition and pH of ocean water.

Fe-bearing green clays (i.e., berthierine, odinite, chamosite, nontronite and glauconite) are the most common early diagenetic clay minerals that form at low and moderate latitudes in both shelf and deep-sea regions (Burst, 1958; Odin and Fullagar, 1988; Wiewióra *et al.*, 2001; Baldermann *et al.*, 2013; Pugliese Andrade *et al.*, 2014). Odin and Fullagar (1988), Mackenzie and Kump (1995), and Pugliese Andrade *et al.* (2014) reported also the rapid low-temperature precipitation of K- and Fe-rich 10 Å and Fe-rich 7 Å phases in nearshore environments.

The transformation reaction occurs, when cations are exchanged between the interlayer space of 2:1 swelling clays and surroundings or due to the reorganization of the clay structure (Eberl, 1984). Experiments on long-term interactions between artificial and/or natural seawaters and dioctahedral swelling clay minerals (smectites and vermiculites), performed by Whitehouse and McCarter (1956) and Carroll and Starkey (1958), indicated that the clays underwent significant changes and transformed into Mg-chlorite or illite-like minerals (or both). Skiba (2013) showed selective adsorption and fixation of K^+ cation by dioctahedral vermiculite from an artificial sea water, which caused transformation of the swelling phases into illite-like phases. On the basis of the experimental saturation of dioctahedral vermiculite with NH_4^+ ions, Skiba *et al.* (2018) suggested the formation of NH_4^+-illite in organic-rich sediments. Studies conducted in natural systems were based on comparison between the clay mineralogy of fresh-water sediments, transported by rivers, and the sediments, deposited in estuaries and within marine environments. In early studies, Grim (1953), Powers (1953, 1957a, b), and Nelson (1958, 1962) suggested that during early diagenesis detrital swelling clay minerals (i.e., dioctahedral smectite and dioctahedral vermiculite) transported by the Patuxent River, the James River, the Rappahannock River (east coast of North America) and the Guadalupe River (the Gulf of Mexico) underwent transformation into Mg-rich chlorite and/or illite. More recently, Hover *et al.* (2002) reported the adsorption of K^+ by high-charge smectite as soon as detrital smectite enters Atchafalaya Bay (Luisiana, U.S.A.). Adsorption continued in the bottom sediments, which was indicated by the depletion of K^+ in the pore waters. Cuadros *et al.* (2017), studying the mangrove soils of the Brazilian coast, showed that the high reactivity of dissolved Fe, Si, Mg, Na and K destabilized and transformed kaolinite into Fe-illite through smectite. Although the transformations occurred at surface temperature, the reactions took place in months, which, in contrast to the formation of Fe-rich clays, such as glauconite or odinite (>10^3 years), is extremely rapid (Velde and Church, 1999; Cuadros *et al.*, 2017).

The available data describe the highly important influence of reverse weathering on the storage of alkaline ions in sediments of moderately and highly saline marine environments, such as the Amazon Delta area or the Gulf of Mexico. The mineralogical sink of dissolved elements in a brackish environment appears to be overlooked, even though a significant amount of potassium was reported as being taken up by high-charge smectite in such an environment (Hover *et al.*, 2002). Mineralogical studies of the clay fractions from temperate and brackish environments certainly will complement knowledge of the elements cycle and the mechanism, leading to the consumption of alkaline ions.

The Vistula River in Poland is the very last unregulated, major European river (Majewski, 2013). The Vistula drainage area for the most part is located in the temperate climate zone. Under such conditions, dioctahedral swelling clays (i.e., smectite and/or vermiculite) form in soils. During heavy rains, the clays are washed from the soils and carried by the Vistula River into Gdańsk Bay, where they are deposited as delta-front and prodelta sediments. The delta front of the Vistula River as a young landform, formed since the end of the nineteenth century, constitutes a unique case for studying early diagenetic reverse weathering. To the knowledge of the present authors, no detailed study into the clay mineralogy and geochemistry of the Vistula loads is available. The clay mineral composition of Gdańsk Bay surface sediments was studied by Stoch *et al.* (1980), who reported the presence of illite, kaolinite, dioctahedral smectite, and chlorite. In the transect from the Vistula mouth toward the Gdańsk Deep, Stoch *et al.* (1980) noted an increasing trend in the content of illite and chlorite and at the same time a decreasing trend in the content of smectite. It was suggested that the smectite might have transformed into chlorite and illite.

The aims of the present study were (1) to determine the detailed clay mineralogy of suspended Vistula River loads and river sediments deposited in Gdańsk Bay and the average layer charge of expandable interlayers likely to be present in those sediments, using the new O-D vibrational spectroscopy method, developed by Kuligiewicz *et al.* (2015a) and (2) to determine if the swelling clays, probably present in the Vistula loads, are stable in the marine environment of the Baltic Sea or if they undergo early diagenetic transformations.

STUDY AREA

Gdańsk Bay is located in the southern part of the Baltic Sea (Fig. 1). The seafloor of the bay is covered by Holocene sands, loamy sands, or clay loam down to approximately the 60 m isobath. In general, the grain size of the sediments

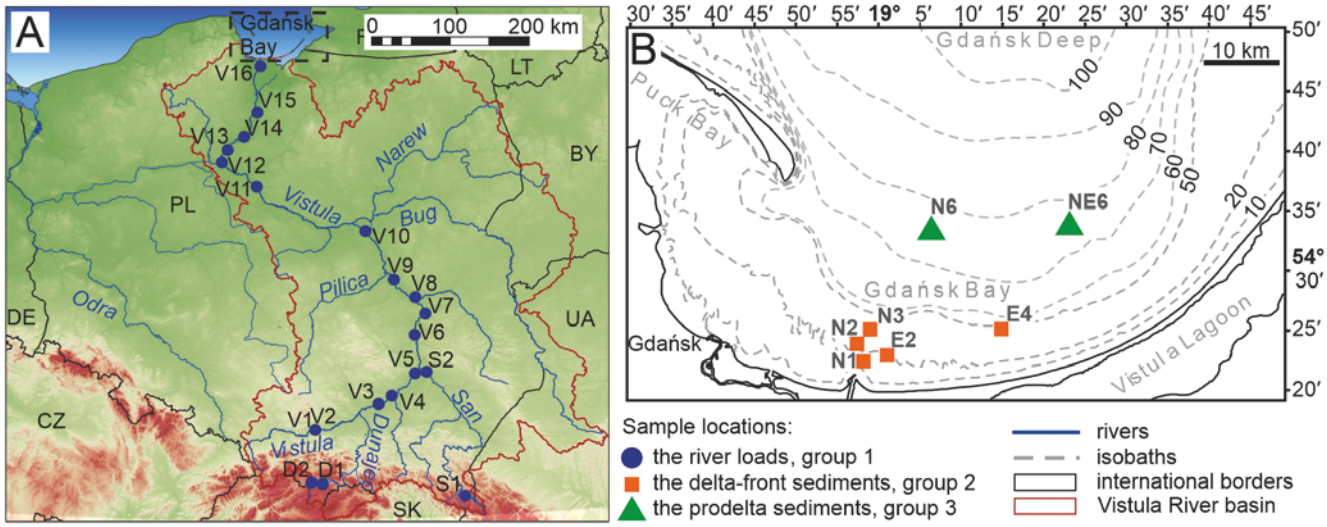

Fig. 1. Maps of study area. **A.** Topography of Poland with the Vistula River basin marked and sampling locations of the rivers loads. The exact coordinates are given in Table 1. **B.** Gdańsk Bay, with marked sampling locations of delta-front seafloor sediments and prodelta cores.

decreases with increasing distance from the coast. The deeper part of the Gdańsk Bay basin is covered by silty clay (i.e., mud; Uścinowicz and Zachowicz, 1993a, b, c). Owing to flocculation processes, mud deposition also takes place in front of the Vistula River mouth (i.e., in the delta front; Uścinowicz *et al.*, 1998). Sediments deposited by the Vistula River in the delta front and prodelta are partially reworked and redeposited in the deeper part of the Gdańsk basin (Damrat *et al.*, 2013). The water in Gdańsk Bay is brackish and has an average salinity of around 7.3‰ (Cyberska, 1990). The salinity of surface water in a transect from the Vistula River mouth toward the center of the Gdańsk basin increased from 1.7 to 7.4‰ (Damrat *et al.*, 2013). The dominant ions in Gdańsk Bay water are Cl^- and Na^+, whereas SO_4^{2-}, HCO_3^-, Mg^{2+}, Ca^{2+}, and K^+ ions occur in much smaller concentrations.

The Vistula River is the main supplier of fresh water and terrigenous material to Gdańsk Bay (Fig. 1). It is the longest Polish river (1,047 km) and the second largest river in terms of the average annual discharge that flows into the Baltic Sea. The drainage basin covers 193,960 km^2. The average flow rate on the Tczew water gauge (35 km up from the river mouth) from 1951 through 2015 was 1,044 m^3 × s^{-1} (Górnik, 2018). According to the Köppen-Geiger Climate Classification, the Vistula River basin is under the influence of two types of climate. The western part is located in a humid temperate climate with warm summers (Cfb) and the eastern part is located in a humid continental climate with warm summers (Dfb; Kottek *et al.,* 2006). For the period 1991–2020, the mean annual air temperature in the basin ranged from 7°C to 9°C and the mean annual precipitation ranged between 450 and 800 mm. The exception was the Carpathian Mountains region in the southern part of the basin, where the mean air temperature ranged from 0.1°C to 7°C and the total annual precipitation reached 1,760 mm at the highest elevations (Institute of Meteorology and Water Management – National Research Institute, 2022). Unlike western European rivers (e.g., the Rhine, the Rhone, and the Seine), the Vistula lost the importance it once had as a navigable river in the 18th century. The lack of river regulation caused the development of sandbanks and sandy islands in the middle part of the basin and reshaped the river channel into braided and braided anastomosing channels (Majewski, 2013). Only short segments of the river were regulated. The most important hydrotechnical construction is a dam, located at Włocławek (675 km down the river flow), with a large reservoir built in the 1960s. Even so, each year the Vistula delivers approximately 1.015 million tons of dragged (i.e., bed load) material into Gdańsk Bay (Emelyanov and Stryuk, 2002). The amount of suspended material delivered into the bay was estimated by Emelyanov and Stryuk (2002) to be between 0.66 and 2.2 mill. t/y.

SAMPLES AND METHODS

For the present study, three groups of samples were collected (Tab. 1; Fig. 1). The first group consisted of 20 samples, including 16 from the Vistula River (V1–V16) and four from the three tributaries of the Vistula: the Biały Dunajec River (D1), the Czarny Dunajec River (D2) and the San River (S1 and S2) (Fig. 1A). The samples were collected between October 2016 and September 2019 under different hydrological conditions. During high flow, when the river carried a larger amount of sediment, suspended loads were collected directly from the river's flow. After the river level fell, freshly deposited muds were collected. During the low river stage, sandy mud was taken from the sandbanks. The second group consisted of five samples of seafloor sediments from the Vistula delta front (Fig. 1B), which were taken with a box-corer from the deck of the Oceania vessel during the winter 2012 campaign along two transects, one to the north (N1–N3) and to the east from the river mouth (E2 and E4; Damrat *et al.*, 2013). The third group included two cores (N6 and NE6), collected 75 m below sea level from the prodelta using a gravity corer with plastic inline pipes (KC Denmark, Ø 90 mm, Silkeborg, Denmark Fig. 1B). Core N6 was collected 23 km from the Vistula mouth and

Table 1

Location and type of collected samples.

Sample	Latitude (N)	Longitude (E)	Type of the sediments	Date of fileld work
D1	49.4267	20.0273	suspended loads	29-Apr-17
D2	49.4341	19.8555	suspended loads	29-Apr-17
S1	22.5252	49.2017	sandy mud	14-Apr-19
V1	50.0538	19.9286	suspended loads, freshly deposited mud	07-Oct-16
V2	50.0538	19.9286	sandy mud	25-Sep-17
V3	50.3248	21.0756	suspended loads	30-Oct-17
V4	50.4277	21.3304	suspended loads	30-Oct-17
V5	50.6743	21.7575	suspended loads	30-Oct-17
S2	50.6737	21.9287	suspended loads, freshly deposited mud	30-Oct-17
V6	51.1133	21.7956	sandy mud	30-Oct-18
V7	51.3515	21.9809	sandy mud	30-Oct-18
V8	51.5565	21.8282	sandy mud	30-Oct-18
V9	51.7619	21.4306	sandy mud	30-Oct-18
V10	52.3717	20.9073	freshly deposited mud	16-May-19
V11	52.8786	18.8359	sandy mud	10-Sep-19
V12	53.1417	18.1708	sandy mud	11-Sep-19
V13	53.3050	18.3293	sandy mud	11-Sep-19
V14	53.4320	18.5912	sandy mud	11-Sep-19
V15	53.7447	18.8551	sandy mud	11-Sep-19
V16	54.2568	18.9467	suspended loads, freshly deposited mud	11-Apr-17
N1	54.4168	19.2483	seafloor sand	10-Jan-12
N2	54.3999	18.9587	seafloor sand	10-Jan-12
N3	54.4164	18.9849	seafloor sand	10-Jan-12
E2	54.3929	18.9957	seafloor sand	10-Jan-12
E4	54.4168	19.2483	seafloor sand	10-Jan-12
N6	54.5482	19.1131	mud	Jan-12
NE6	54.5455	19.3849	mud	Jan-12

was 247 cm long, whereas core NE6 was collected 35 km from the Vistula mouth and was 115 cm long. Shells picked from four depths of the N6 core were C-14 dated. The liquid scintillation counting technique was used in the Laboratory of Absolute Dating (MKL, Kraków, Poland), using a HIDEX 300SL spectrometer (Hidex, Turku, Finland). OxCal software (version 4.2.3) was used to calibrate radiocarbon dates against the international calibration curve (IntCal13). Because of the small amount of the material in single 1-cm-thick part of the cores, the cores collected (group 3) were sectioned into ~10 cm intervals. All samples collected were dried at 60 °C for 24 h and gently pre-ground in a steel mortar to pass through a 0.4 mm sieve. The pH was measured in deionized water (1:1 sample:water ratio), using a calibrated pH meter (Elmetron CP-411, Zabrze, Poland) after being equilibrated for 24 h.

Because most of the swelling clays carried by the Vistula River and the products of their potential transformations were expected to be clay-sized, both <2 μm and <0.2 μm (hearafter fine) clay fractions were separated with a Sorvall™ ST 40 Centrifuge (Thermo Scientific™, Waltam, MA, USA) after application of the chemical pretreatments, described by Jackson (1969). Carbonate cements were removed with a Na acetate-acetic acid buffer at pH ~5.5. Organic matter was removed by hydrogen peroxide, buffered with a Na-acetate buffer, and free Fe oxides were removed by the sodium dithionite-citrate-bicarbonate treatment (Mehra and Jackson, 1958). Samples of suspended materials carried by the Vistula River during the high stage of water were analyzed without size separation, owing to the small amount of sediments obtained (5 g or less). Each of the obtained suspensions of the separated clays was split into two portions; one portion was saturated with Na^+ and the other with K^+ using 1 mol × dm^{-3} NaCl and 1 mol × dm^{-3} KCl, respectively. Next, each of the portions was dialyzed, using Nadir® dialysis tubing (pre-washed in de-ionized water to remove glycerol) and dried on a water bath.

High-gradient magnetic separation using a Frantz LB-1 Magnetic Barrier Laboratory Separator (S.G. Frantz CO., INC, Tullytown, PA, USA) was used to separate magnetic

(i.e., Fe-bearing) and nonmagnetic (i.e., Fe-depleted) subfractions from the <2 μm clay fractions for one sample for each group (samples V1, E4, and N6_190) following the procedure given by Tellier *et al.* (1988).

The mineralogy of the separated clays was studied by means of X-ray diffractometry (XRD). Oriented mounts were prepared from Na^+- and K^+-saturated clays by deposition of suspensions of the clays dispersed in deionized water, prepared using a Vibra Cell™ Ultrasonic Liquid Processor (Sonics, VCX 130PB, Newtown, CT, USA) onto petrographic glass slides (with surface density of about 10 mg × cm^{-2}) or silicon low-background wafers (with surface density below 10 mg × cm^{-2}). Randomly oriented mounts also were prepared from selected Na-saturated fine clays by side loading. The XRD patterns for Na^+- and K^+-saturated clays were scanned in air-dried conditions at ambient relative humidity, which ranged from 9–65%. XRD patterns for K^+-saturated clays were also scanned after heating the mounts for 1 h at 330°C and again at 550°C, whereas for Na^+-saturated clay fractions XRD patterns were collected after ethylene-glycol solvation (12 h at 60°C) of the previously air-dried mounts.

A Philips X'Pert diffractometer with a vertical goniometer PW3020 (Philips Electronics N.V., Almelo, The Netherlands) was used for the XRD. The instrument was equipped with a 1° divergence slit, 0.2 mm receiving slit, incident- and diffracted-beam Soller slits, a 1° anti-scatter slit, and a graphite monochromator positioned at the diffracted beam path. CuKα radiation was produced at 40 kV and 30 mA. The random mounts were scanned from 2–65° 2θ at 0.02°/5 s, whereas the oriented mounts were scanned in the range 2–52° 2θ at 0.02°/2 s. The identification of clay minerals was based on the presence of diagnostic reflections in XRD patterns of oriented mounts according to the criteria, given by Barnhisel and Bertsch (1989), Moore and Reynolds (1997), and Środoń (2006).

Fourier transform infrared spectroscopy (FTIR) was used to characterize clay minerals. The identification of the bands, present on collected spectra was based on the work of Russel and Fraser (1994). Moreover, the collected spectra were used to calculate the average layer charges (LC) of expandable interlayers by means of the O-D vibrational spectroscopy method, described in detail by Kuligiewicz *et al.* (2015a, b) for D_2O saturated dioctahedral smectites. Positions of the high-frequency O-D stretching band (hereafter νO-D) are linearly correlated with the layer and interlayer charges, established against the structural formula method (SFM) and the alkylammonium method, respectively. Because of the expected abundance of a variety of swelling clay minerals, prediction of LC was based on the equation, obtained from linear correlation of νO-D and SFM. The error of the returned value is estimated to 0.02 per formula unit (p.f.u.). The analyzed clay fraction was saturated with Na^+ ions. Infrared spectra were collected in the range 4000–400 cm^{-1} as a 100-scan averages with 4 cm^{-1} resolution, using a Thermo Nicolette™ Is50 spectrometer (Thermo Scientific, Waltam, MA, USA), equipped with the PIKE MIRacle™ single-reflection attenuated total reflectance (ATR) accessory (diamond crystal), and a custom designed D_2O-saturation system. Measurements were performed in a dry atmosphere of N_2 (Air Products, purity >98 vol%, <0.02 ppb H_2O), after saturation of the samples with D_2O (Deutero, 99.9 atom% D, Kastellaun, Germany).

To determine the major-element geochemistry of the separated clays, the samples were digested (mineralised) in a mixture of spectrally clean and concentrated nitric, hydrochloric, and hydrofluoric acids in the presence of boric acid, using the Ethos-Up Milestone microwave oven (Milestone Srl, Sorisole (BG), Italy). A Spectro Arcos (ICP-OES) spectrometer (SPECTRO Analytical Instruments GmbH, Kleve, Germany) with the radially side-on viewed torch configuration was used for the elemental analyses. Certified reference material OREAS 920 (Oreas®, Melbourne, Australia) was processed and measured in the same way as the samples in the same analytical cycle to monitor the accuracy of the analyses. The statistical significance of the differences in chemical composition of the <0.2 μm clay fraction between studied groups of samples were calculated, using the non-parametric Kruskal-Wallis H test (Kruskal and Wallis, 1952). The post-hoc Dunn's multiple comparisons test (Dunn, 1964) was used to determine which studied groups differ ($p \leq 0.05$). All the calculations were performed using STATISTICA 13 software.

RESULTS

Radiocarbon ages of prodelta sediments

The shells, obtained from the 187 cm, 117 cm, 93 cm, and 66 cm depths of the N6 core, were dated to cal BC 407–235 (95%), cal AD 661–863 (95%), cal AD 770–952 (95%), and cal AD 984–1030 (95%), respectively. Therefore, the sediments studied were deposited most likely since the 5th Century BC.

pH of the sediments

Bulk rock material of the Vistula River loads showed alkaline pH values, ranging between 7.0 and 8.5. Similar pH values (6.7–7.4) were measured for the delta-front sediments (group 2), whereas samples from the two cores (group 3) gave pH values between 2.5 and 7.18 (Tab. 2).

Mineral composition of clay fractions

The <0.2 μm fractions separated from the Vistula River loads and from the delta-front sediments were dominated by smectite-rich mixed-layered illite-smectite (Ilt-Sme). They also contained kaolinite and illite (Figs 2, 3). Most of the smectitic components, present in the <0.2 μm fractions, separated from the river sediments, collapsed to ~10 Å under air-dried condition after K-saturation (Fig. 2). XRD patterns of the air-dried K-saturated <0.2 μm clays from the delta front samples showed ~14 Å reflections, which collapsed after heating the mounts at 330˚C (Fig. 3). According to Barnhisel and Bertsch (1989), Meunier (2007), Lanson *et al.* (2015), and Dietel *et al.* (2019) this might indicate the presence of hydroxy-interlayered minerals (HIMs). The <0.2 μm clay fractions, separated from the cores collected from the Vistula prodelta, contained chlorite, illite,

Table 2

Chemical properties of analyzed clay fractions.

Sample	pH [1]	Measured fraction[2]	LC[3]	Fe_2O_3[4]	K_2O	MgO	Al_2O_3	Na_2O	SiO_2	TiO_2
Group 1 – the rivers loads										
D1	n.a.	s.m.	0.52	5.43	2.77	2.34	14.03	0.98	52.20	0.67
D2	n.a.	s.m.	0.52	n.a.	n.a.	n.a.	n.a.	n.a.	n.a.	n.a.
S1	n.a.	<2	0.47	5.50	5.07	3.02	23.79	0.79	47.06	0.88
S1	n.a.	<0.2	n.a.	2.24	3.34	1.21	23.42	1.10	45.35	0.49
V1	8.42	<0.2	0.52	5.46	2.64	2.04	21.53	1.58	43.64	0.48
V2	7.42	<0.2	n.a.	n.a.	n.a.	n.a.	n.a.	n.a.	n.a.	n.a.
V3	n.a.	s.m.	0.50	3.39	2.67	1.49	14.82	1.47	62.68	0.75
V4	n.a.	s.m.	0.48	3.49	2.57	1.53	15.05	1.48	60.97	0.68
V5	n.a.	s.m.	0.51	3.83	2.75	1.72	16.37	1.48	54.98	0.71
S2	n.a.	s.m.	0.49	3.39	2.60	1.51	14.45	1.52	62.04	0.72
S2	n.a.	<0.2	0.48	8.43	2.28	2.32	18.83	1.77	48.99	0.60
V6	8.35	<2	0.48	6.15	2.72	1.94	18.60	0.76	47.70	0.71
V6	8.35	<0.2	0.48	6.70	2.66	2.09	19.64	1.09	45.99	0.74
V7	7.90	<2	0.49	6.38	2.75	1.89	18.15	1.09	49.20	0.73
V7	7.90	<0.2	0.48	6.86	2.61	2.06	19.26	1.42	48.13	0.70
V8	8.50	<2	0.51	6.63	2.54	1.82	17.56	0.78	47.49	0.76
V8	8.50	<0.2	0.51	8.25	2.39	1.94	19.26	1.26	48.13	0.73
V9	8.30	<2	0.50	6.62	2.83	2.04	19.26	1.01	49.42	0.72
V9	8.30	<0.2	0.49	7.16	2.65	2.04	18.87	1.25	48.56	0.77
V10	7.75	<0.2	0.48	6.32	2.88	2.26	21.15	1.33	47.49	0.53
V11	8.36	<2	n.a.	n.a.	n.a.	n.a.	n.a.	n.a.	n.a.	n.a.
V12	8.33	<2	0.51	n.a.	n.a.	n.a.	n.a.	n.a.	n.a.	n.a.
V12	8.33	<0.2	0.49	9.09	2.36	1.87	18.77	1.11	47.49	0.67
V13	8.43	<2	0.48	7.13	2.70	1.92	18.34	0.66	51.77	0.68
V13	8.43	<0.2	0.51	6.98	2.14	1.74	17.47	1.47	46.42	0.60
V14	7.95	<2	0.47	5.86	2.75	1.91	18.88	0.97	50.91	0.71
V14	7.95	<0.2	0.46	8.42	2.39	2.07	19.64	1.78	48.13	0.61
V15	8.14	<2	0.51	6.48	2.60	1.87	17.77	0.45	49.42	0.66
V15	8.14	<0.2	0.51	8.00	2.39	1.89	17.83	1.50	48.35	0.68
V16	6.96	<0.2	0.50	7.75	2.42	2.01	19.64	1.75	44.71	0.47
Group 2 – the seafloor sediments from the Vistula delta front										
N1	7.36	<0.2	0.56	6.02	2.28	2.21	16.22	4.45	48.77	0.52
N2	7.20	<0.2	0.48	7.83	3.25	2.24	18.87	1.29	48.13	0.59
N3	6.70	<0.2	0.51	7.39	3.11	2.11	17.07	1.10	45.35	0.48
E2	n.a.	<0.2	0.50	7.82	3.28	2.22	18.43	1.35	47.28	0.55
E4	7.12	<0.2	0.56	7.43	2.58	2.09	18.09	3.15	41.50	0.42
Group 3 – core sampled from prodelta sediments										
N6_1	6.90	<0.2	0.50	8.03	3.63	2.8	19.07	1.43	49.63	0.62
N6_31	6.66	<0.2	0.47	8.43	3.58	2.84	19.07	1.21	45.35	0.46
N6_51	6.56	<0.2	0.46	8.62	3.70	2.90	18.88	1.15	45.14	0.48
N6_71	5.60	<0.2	0.46	8.58	3.76	2.92	18.62	0.98	44.50	0.51
N6_91	5.64	<0.2	0.46	8.55	3.84	2.93	18.70	1.10	45.14	0.48
N6_106	7.11	<0.2	0.49	8.02	3.67	2.84	18.30	1.91	44.71	0.50

Sample	pH [1]	Measured fraction[2]	LC[3]	Fe_2O_3[4]	K_2O	MgO	Al_2O_3	Na_2O	SiO_2	TiO_2
N6_121	6.67	<0.2	0.47	8.03	3.78	2.92	19.26	1.16	47.06	0.57
N6_141	7.18	<0.2	0.46	8.06	3.64	2.84	18.05	1.06	44.50	0.52
N6_171	7.03	<0.2	0.46	8.55	3.60	2.84	18.79	1.24	46.42	0.52
N6_190	6.80	<0.2	0.48	8.21	3.69	2.92	18.88	1.13	45.56	0.52
NE6_1	4.33	<0.2	0.50	8.06	3.12	2.42	18.43	1.58	42.57	0.42
NE6_11	2.50	<0.2	0.48	8.22	3.47	2.60	19.26	1.47	45.99	0.47
NE6_30	3.00	<0.2	0.48	8.08	3.32	2.60	18.20	1.35	44.07	0.46
NE6_51	6.17	<0.2	0.48	7.95	3.54	2.75	18.79	1.32	45.14	0.47
NE6_70	5.95	<0.2	0.48	7.73	3.41	2.67	17.60	1.42	41.50	0.44
NE6_91	5.62	<0.2	0.48	8.31	3.72	2.89	18.88	1.34	45.78	0.46
NE6_106	2.81	<0.2	0.48	8.38	3.54	2.75	18.28	1.44	44.50	0.44

[1] pH (H_2O) measured for bulk rock
[2] fractions in µm
[3] average layer charge of swelling phases [per formula unit]
[4] content of oxides measured by ICP-OES [wt%]
s.m. – suspended material
n.a. – not analyzed

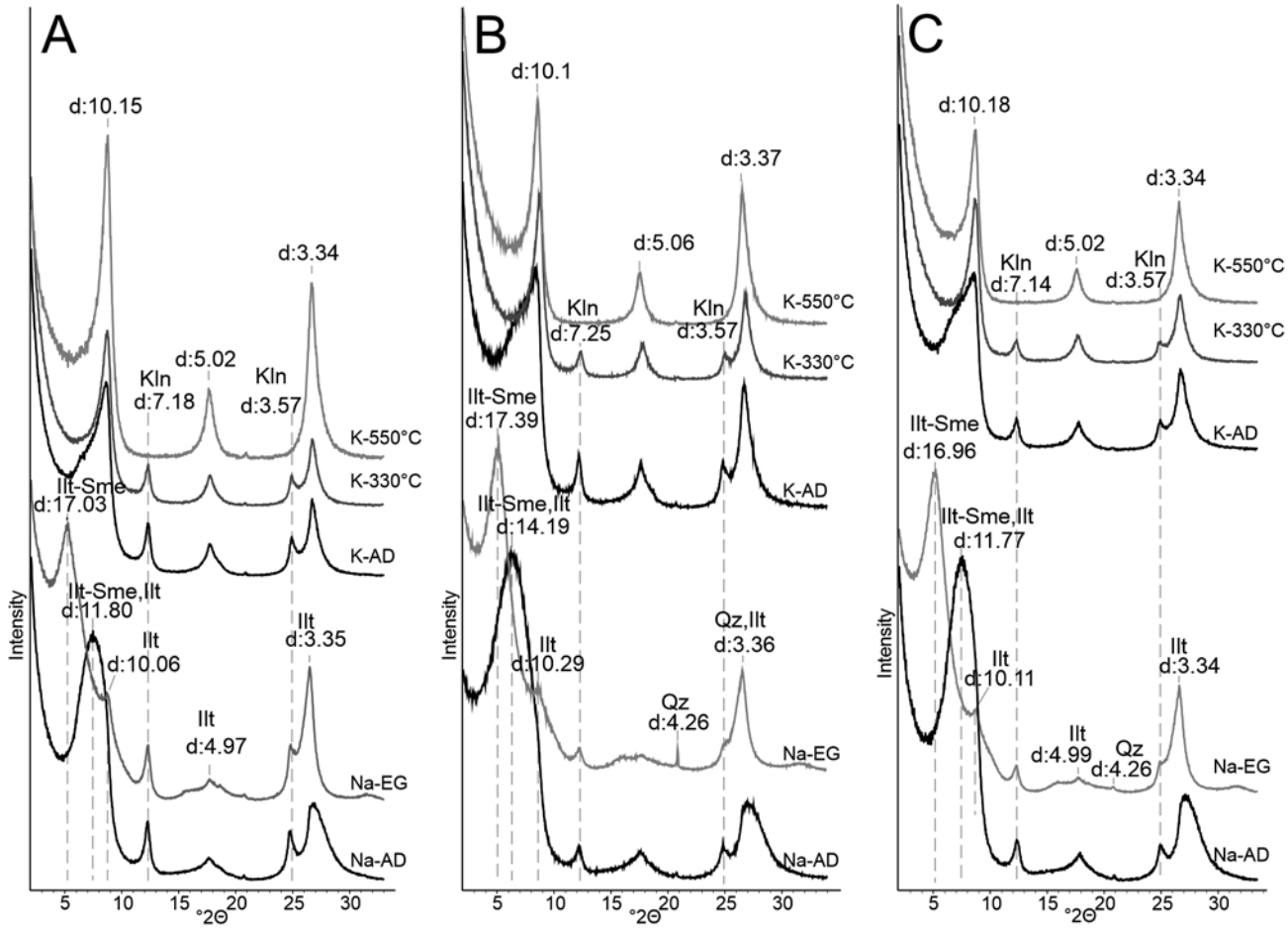

Fig. 2. Selected XRD patterns of oriented mounts of Na- and K-saturated clay fractions <0.2 µm. **A.** the clays separated from sample V1. **B.** the clays separated from sample V10. **C.** the clays separated from sample V16. Abbreviations: AD – air-dried condition, EG – ethylene glycol solvated, RH – relative humidity, Ilt – illite, Ilt-Sme – smectite-rich illite-smectite mixed layered minerals, Kln – kaolinite, Qz – quartz.

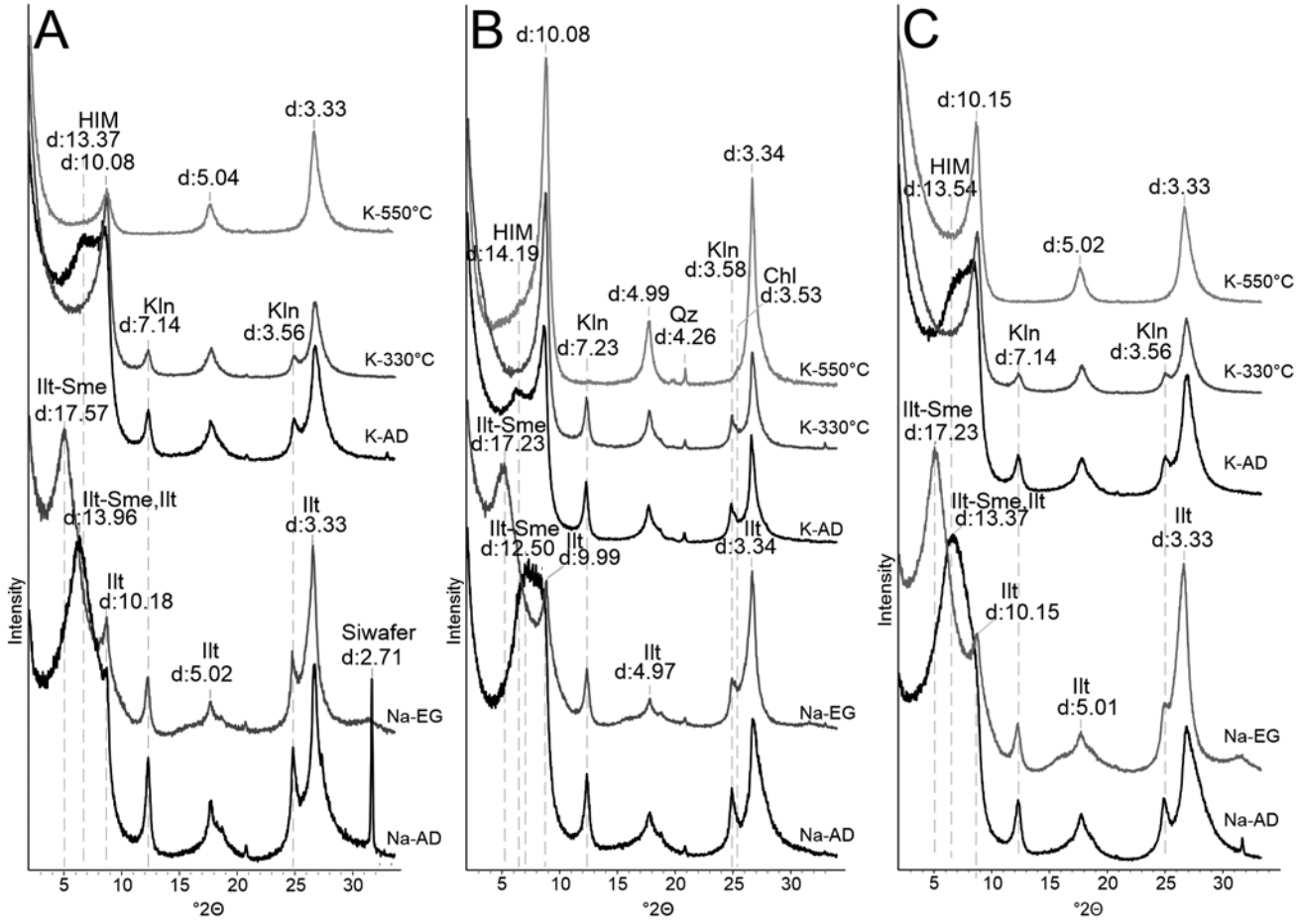

Fig. 3. Selected XRD patterns of oriented mounts of Na- and K-saturated clay fractions <0.2 μm separated from the delta-front sediments. **A.** N1 sample. **B.** E2 sample. **C.** E4 sample. Abbreviation: HIM – hydroxy interlayered minerals.

Ilt-Sme, and kaolinite. They were depleted in smectite-rich Ilt-Sme and enriched in illite, compared to the <0.2 μm clay fractions from the river loads and the delta-front sediments (Fig. 4). Kaolinite contents of the <0.2 μm clay fractions were similar in all of the collected samples (Figs 2–4). Fine clays, separated from both prodelta cores, contained chlorite, as indicated by the presence of ~14 Å XRD reflection after heating the mounts at 550 °C (Fig. 4B).

The <2 μm fraction, separated from all groups of samples, contained Ilt-Sme, illite, kaolinite, and traces of chlorite. Chlorite was present in the <2 μm fractions, separated from the S1 sample (river load collected in the upper San River basin. encompassing part of the Carpathian Mountains; Fig. 5A); the V6 and V7 (river loads collected in the middle Vistula Basin); and the V13 and V15 samples (river load collected in the lower Vistula Basin; Fig. 5B). A trace of chlorite was also identified in the <2 μm fraction of the N3 delta-front sample (Fig. 5C). Chlorite was evident in all the <2 μm clay fractions, separated from both cores studied. Chlorite was also present in the coarsest samples, collected as suspended material during a flood in the upper Vistula basin (D1, D2, V3, V4, V5; Fig. 6).

XRD patterns of random mounts showed broad reflections between ~1.502 Å and 1.507 Å in the 060 region, which indicates that the predominant clay minerals are dioctahedral (Fig. 7). The magnetic subfractions, separated from the V1 and E4 samples, contained smectite-rich Ilt-Sme, illite, kaolinite, and chlorite (Fig. 8A, B). XRD patterns of the magnetic subfractions of the V1 sample showed the additional presence of chlorite-vermiculite or chlorite-smectite (or both) mixed-layered clay minerals (Fig. 8A), as indicated by the ~12 Å reflection in patterns, registered after heating the mounts at 330 °C. The magnetic subfraction, separated from the bottom of the N6 core, was enriched in chlorite and significantly depleted in smectite-rich Ilt-Sme, relative to the magnetic subfractions of clays from the Vistula River loads and the delta-front seafloor sediments (Fig. 8C). Non-magnetic subfractions (tailing) from the Vistula River loads and from the delta-front sediments contained smectite-rich Ilt-Sme and kaolinite, whereas tailings from prodelta sediments were composed of illite, kaolinite, and only traces of smectite-rich Ilt-Sme.

FTIR SPECTRA AND AVERAGE LAYER CHARGES OF SWELLING MINERALS

FTIR spectra, collected for all samples, showed patterns typical for dioctahedral 2:1 clay minerals, with stretching AlAl-OH bands at ~3620 cm^{-1} and the bending bands near 910 cm^{-1} (Fig. 9). Strong bands at ~1000 cm^{-1} were most likely due to Si-O stretching vibrations. Some of the clays from

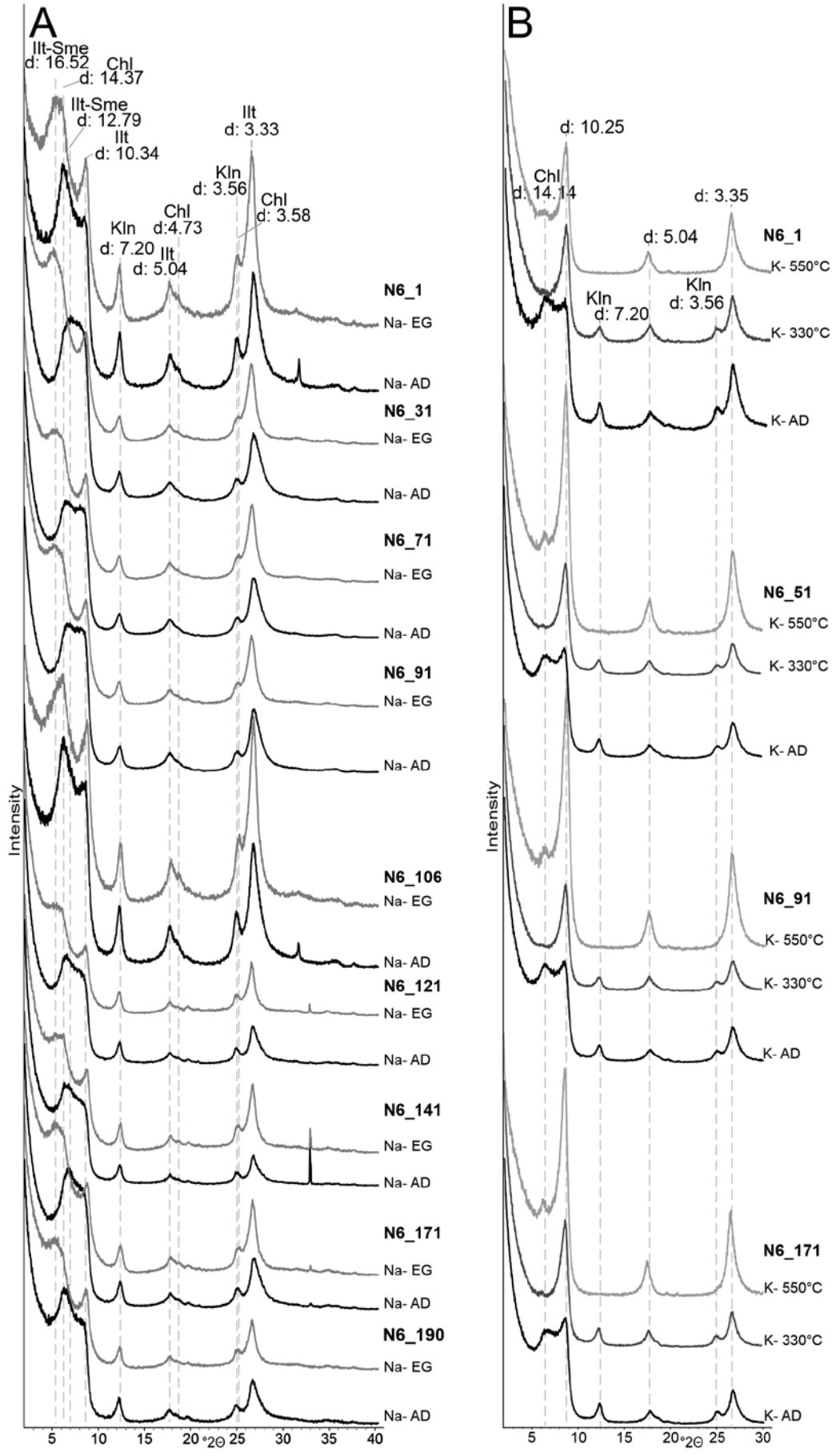

Fig. 4. XRD patterns of oriented mounts of clay fraction <0.2 μm separated from the N6 core. **A.** selected XRD patterns of Na-saturated samples. **B.** selected XRD patterns of K-saturated samples. Abbreviation: Chl – chlorite.

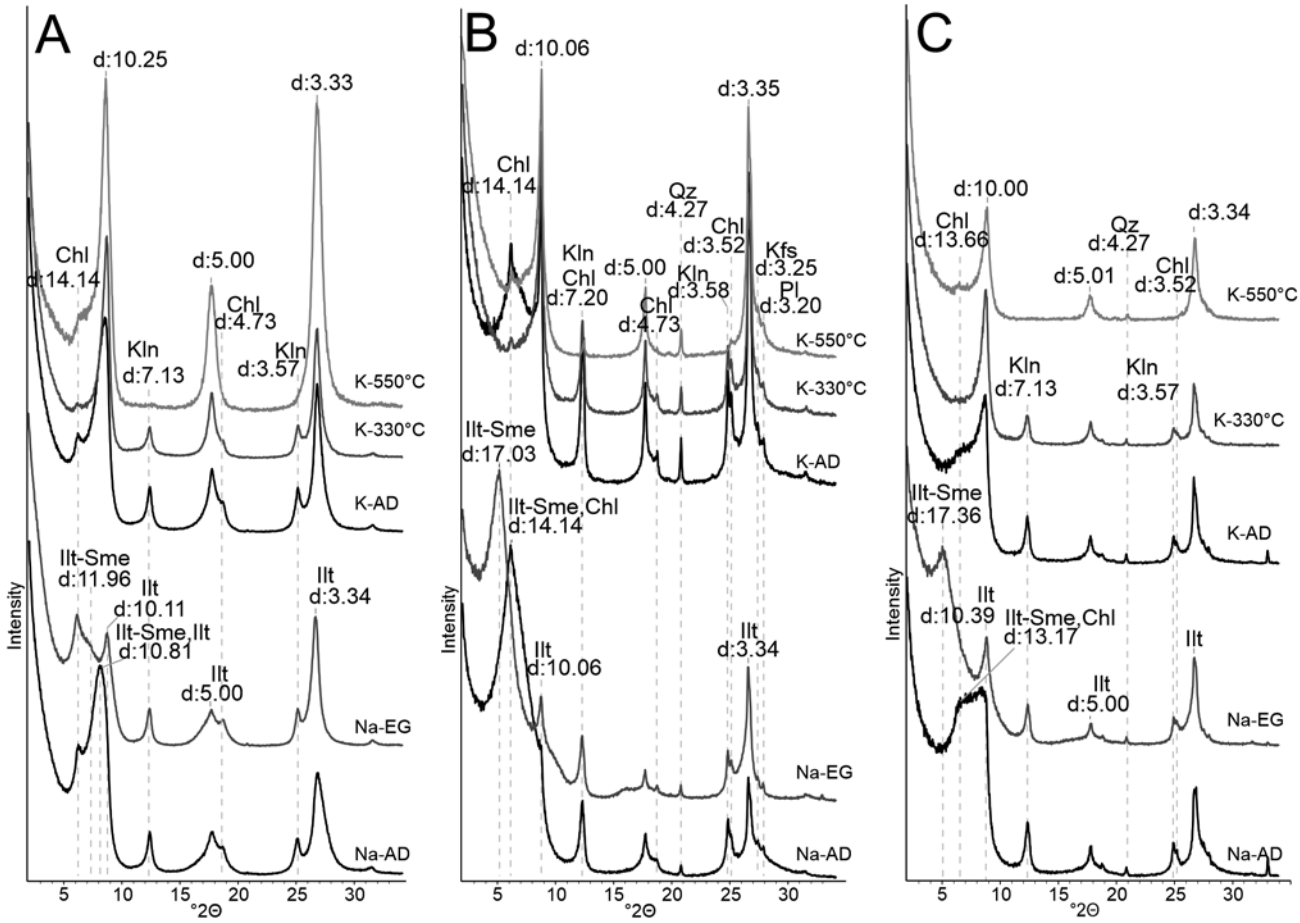

Fig. 5. Selected XRD patterns of oriented mounts of Na- and K-saturated clay fraction <2 µm. **A.** The clays separated from S1 sample (the mud collected from the bank of the San River's tributary). **B.** the clays separated from V15 sample (sand collected at the Vistula River bank). **C.** the clays separated from N3 sample. Abbreviations: Kfs – K-feldspars, Pl – plagioclase.

the Vistula River loads showed higher Al for Si substitution in the tetrahedral sheet, as indicated by the bands near 980 cm^{-1} (Fig. 9). Weak 830cm^{-1} bands may originate from Al-O out-of-plane vibrations in the smectitic component and/or AlMg-OH deformation vibrations in illite, whereas bands at 750 cm^{-1} were assigned to AlSi-O in-plane vibrations in illite in the Ilt-Sme structure. Bands at 3697 cm^{-1}, and some of the intensity of 3620 cm^{-1} bands, were interpreted as indicating the presence of kaolinite. Doublets at 798 cm^{-1} and at 778 cm^{-1} were detected on the spectra of clay fractions from the Vistula River loads and the delta-front samples, indicating admixtures of quartz. The exchange of interlayer H_2O with D_2O and the associated "shift" of stretching vibrations of adsorbed heavy water toward lower wavenumbers in the case of chlorite-containing clays "uncovered" a doublet at ~3560 cm^{-1} and at ~3430 cm^{-1}. These bands indicated a probable trioctahedral character of the octahedral sheet within the interlayer space of the chlorite (Russell and Fraser, 1994; Schroeder, 2002). The octahedral sheets in the 2:1 layers of the chlorite appeared to be dioctahedral, as indicated by the dominating AlAl-OH band at ~3620 cm^{-1} (Fig. 9).

All spectra of the studied clay fractions saturated with D_2O showed the O-D stretching envelope at 2200–2800 cm^{-1}. The position of νO-D ranged between 2687 and 2690 cm^{-1}. The LC calculated ranged between 0.46 and 0.56 p.f.u. (Tab. 2). The highest LCs (above 0.50 p.f.u.) were measured for the clays from the delta front sediments and from the Vistula River loads, regardless of the analyzed fraction (Tab. 2). The LC of expandable interlayers from N6 and NE6 cores were lower than the LC of the clays from the Vistula loads and from the delta- front sediments and did not exceed 0.50 p.f.u. (Tab. 2).

CHEMICAL COMPOSITION OF CLAY FRACTION

All samples exhibited high SiO_2 and Al_2O_3 contents (41.5–62.68 wt% and 14.03–23.79 wt%, respectively) (Tab. 2), which is consistent with the dominance of dioctahedral aluminosilicates in the clays studied. The content of K_2O, MgO, and Fe_2O_3 in clay fraction <0.2 µm from the Vistula River loads, the delta-front sediments, and separately from the N6 and NE6 core samples, was compared. The Kruskal-Wallis test showed that there was a significant difference in the content of those oxides in the groups studied (Tab. 3). The post-hoc test indicates that the contents of the oxides were significantly higher (for the $p \leq 0.05$) in the clay fraction from N6 core than contents of the oxides in the clay fraction from the other two groups of samples.

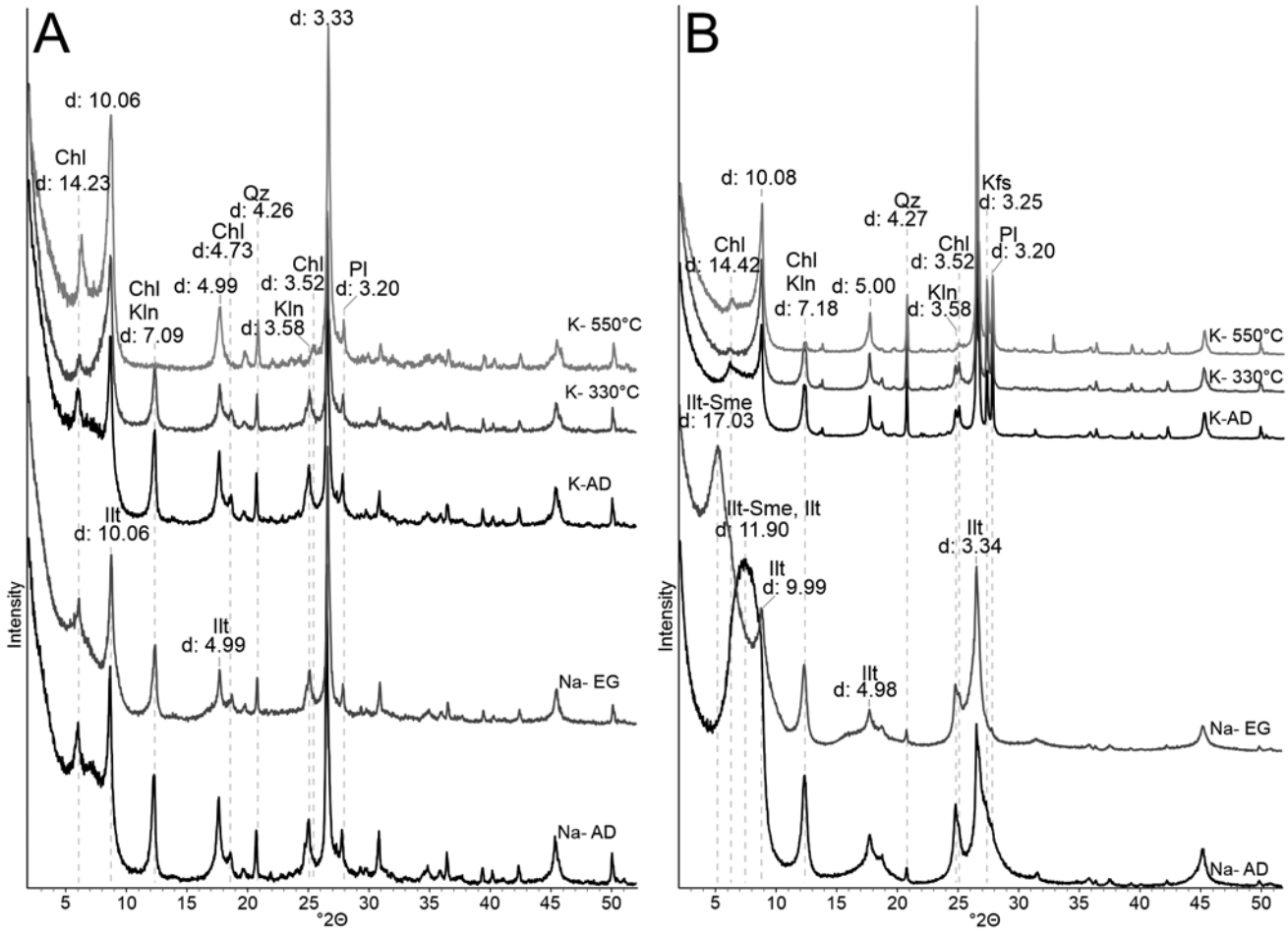

Fig. 6. Selected XRD patterns of oriented mounts of Na-saturated and K-saturated suspended material. **A.** D1 sample (collected from the Biały Dunajec River current). **B.** V5 sample (collected from the Vistula River current).

Table 3

The Kruskall-Walias test result of differences between studied groups of samples in K_2O, MgO, Fe_2O_3 content and LC measured for clay fraction <0.2 um.

Oxide	H-statistic	Degree of freedom	Number of samples	p-value
K_2O	26.74	3	35	<0.0001
MgO	28.86	3	35	<0.0001
Fe_2O_3	11.74	3	35	0.0081
LC	14.53	3	34	0.0023

The clay fraction from the NE6 core samples had significantly (for the $p \leq 0.05$) higher content of MgO and Fe_2O_3 than the clay fraction from the Vistula River and delta-front samples (Fig. 10). The median values of the content of the MgO and Fe_2O_3 within Vistula River loads were higher in both clay fractions than in the suspended material. The median value of K_2O within the Vistula River loads was, on the other hand, the lowest in the fraction <0.2 μm and higher in the fraction <2 μm and suspended material (Fig. 10).

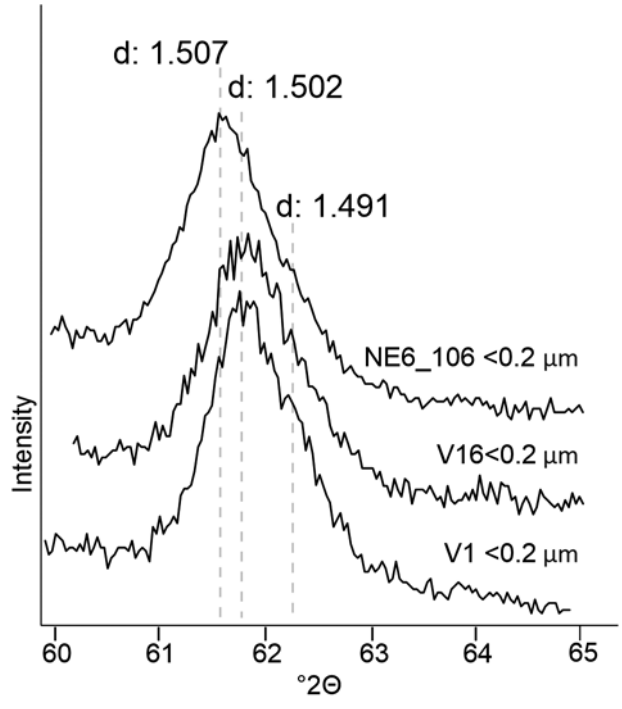

Fig. 7. The 060 region of XRD patterns of random mounts representative for studied samples.

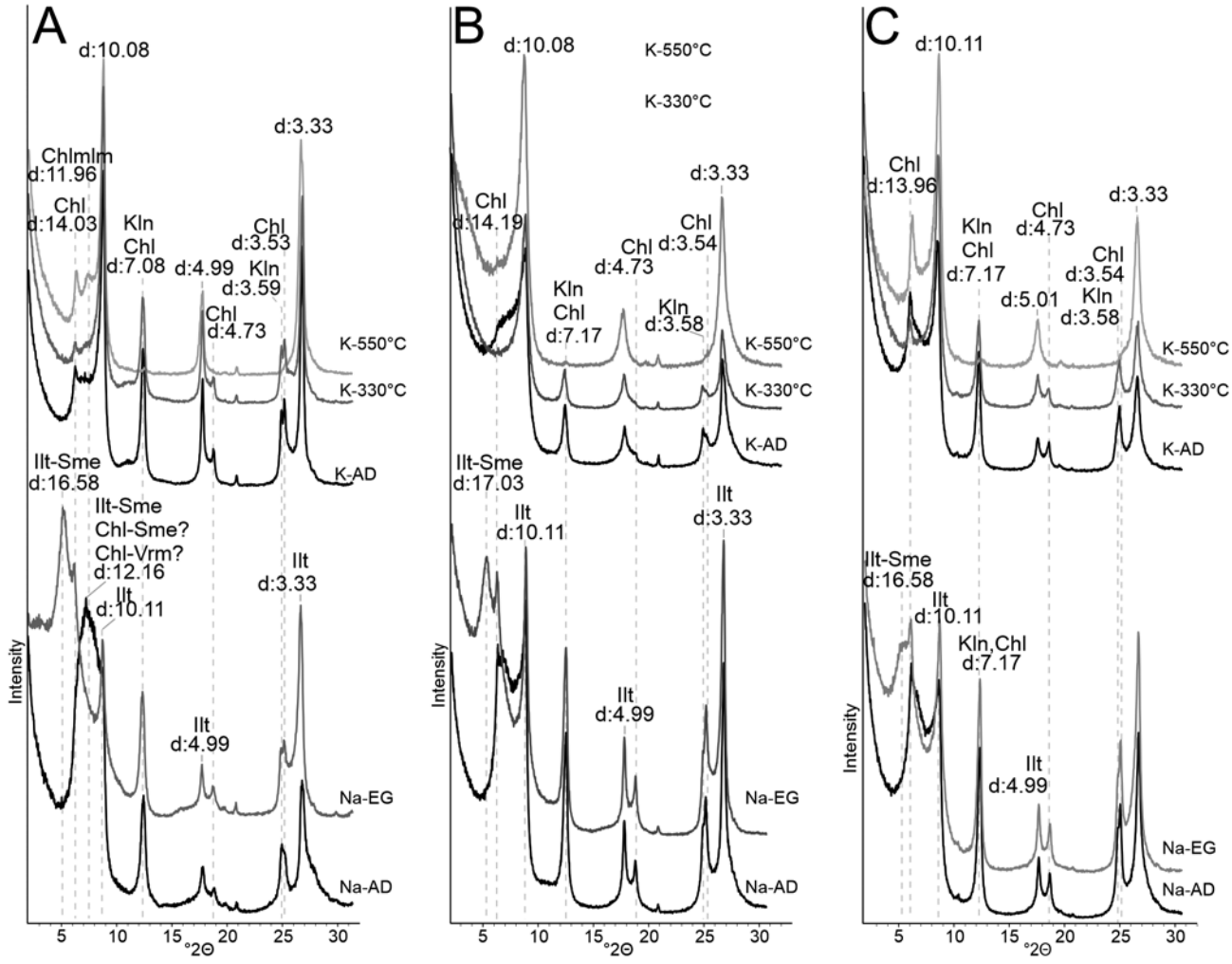

Fig. 8. The selected XRD patterns of oriented mounts of Na- and K-saturated magnetic subfraction separated from <2 μm clay fraction. **A.** The subfraction separated from sample V1. **B.** The subfraction separated from E4 sample. **C.** the subfraction separated from sample N6_190. Abbreviations: Chlmlm – chlorite mixed-layered minerals.

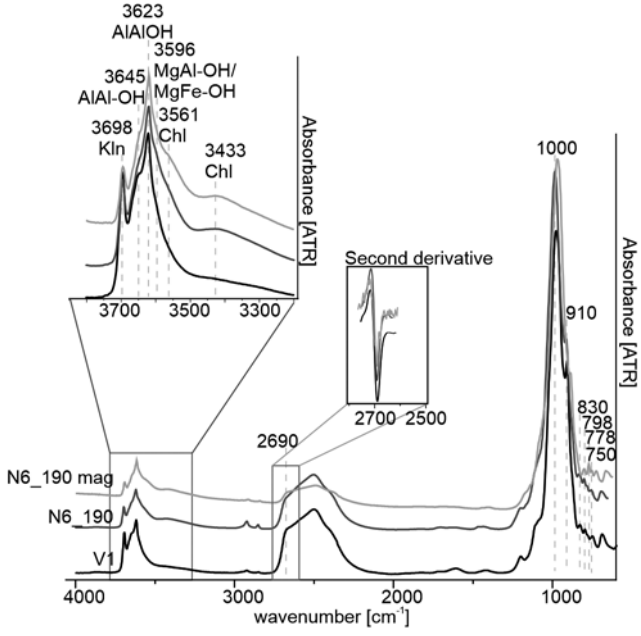

Fig. 9. ATR-IR spectra of selected clay fractions saturated with D_2O with zoom in of OH-stretching region and 2nd derivative used for determination of high-frequency O-D stretching band position.

DISCUSSION

The Vistula basin encompasses high mountains, highlands and lowlands that are affected by slightly different weathering conditions. Therefore, the mixture of clay mineral particles, carried in the Vistula loads, represented different degrees of chemical weathering, reflected in the diversified chemical composition and the measured layer charge of the fine clay fraction. The both clay fractions were dominated by Ilt-Sme. As shown by Kuligiewicz *et al.* (2018), the O-D method probes the LC of only expendable interlayers and the presence of collapsed ones does not bias the results. Therefore, the method can be used for the prediction of the LC of the expandable component of mixed-layered clay minerals (Fig. 11). On the basis of the criteria given by Christidis and Eberl (2003), smectite with a layer charge >0.426 p.f.u. can be designated as a high-charged mineral. Therefore, the obtained LCs of the samples studied showed that the smectitic component of Ilt-Sme is a high-charged smectite. The mixture of clays in the river loads also contained kaolinite and illite. Traces of chlorite were present in the clay fraction <2 μm separated from the five samples. A relatively higher amount of chlorite was carried

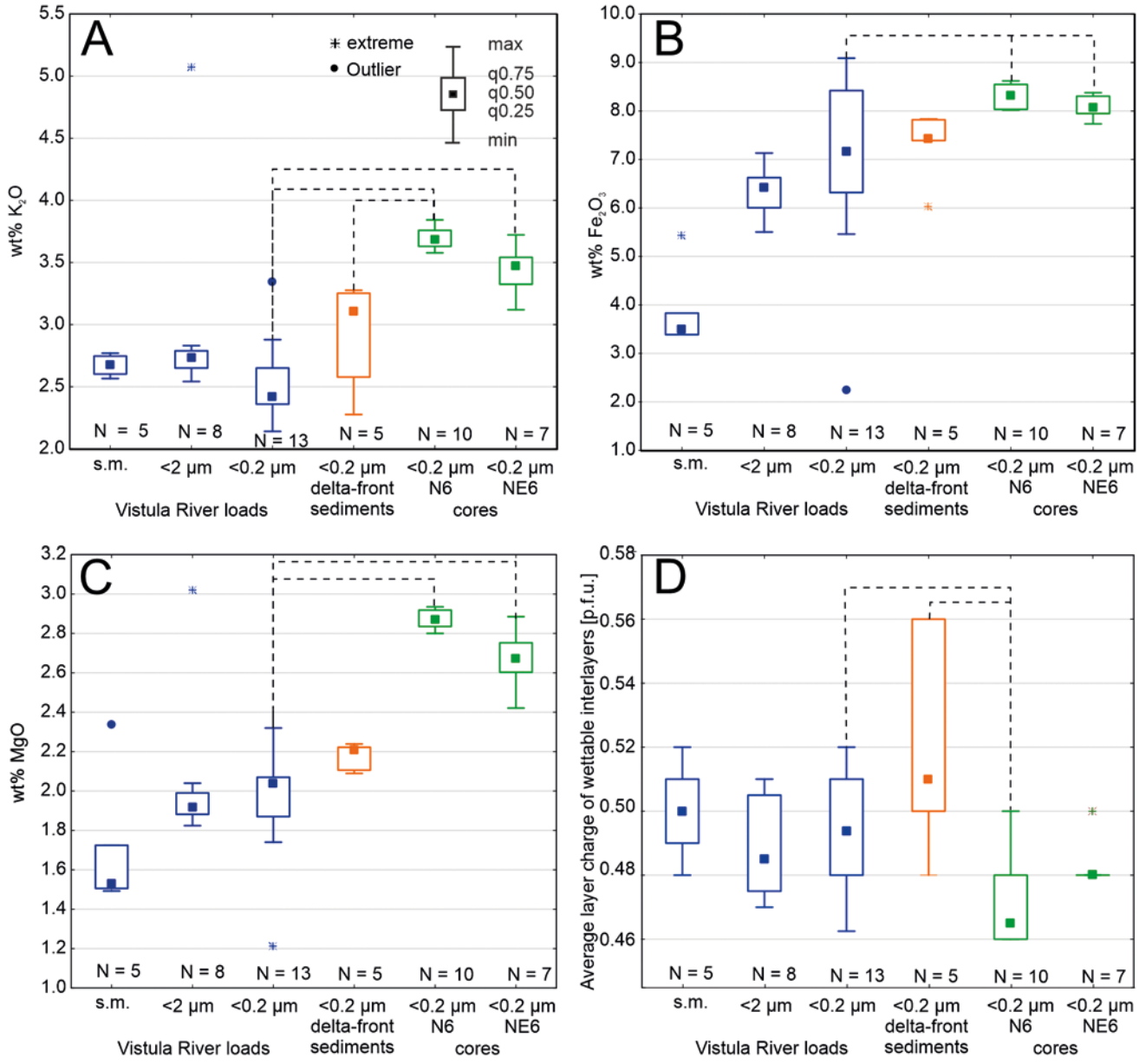

Fig. 10. The quartiles (q) of distribution of selected parameters of studied samples. **A.** K_2O (wt%). **B.** Fe_2O_3 (wt%). **C**. MgO (wt%). **D.** Average layer charge of expandable interlayers (p.f.u.). The dashed lines pair the groups with statistically significant ($p \leq 0.05$) difference in the content of given oxides. Abbreviations: s.m. – suspended material, N – number of analyzed samples.

in the suspended material than in the clay fraction, separated from the sediments of the river. A trace amount of interstratified chlorite-vermiculite and/or chlorite-smectite also might have been carried by the Vistula River, as indicated by its presence in the magnetic subfraction, separated from the clay fraction of sample V1.

The similarity of the clay mineral assemblages, recognized within the delta-front and prodelta sediments, strongly indicated detrital input as the major process that shapes the clay mineral composition within the studied bay. However, the distribution of Ilt-Sme, illite, kaolinite and chlorite in the part of Gdańsk Bay studied did not correspond with the model proposed by Chamley (1989). As claimed by Chamley (1989), smectite generally settles less rapidly than illite, chlorite and kaolinite, so it is expected that smectite is concentrated in the more distal sediments. In the present study, the fine clays, separated from prodelta sediments (samples from N6 and NE6 cores), were depleted in smectite-rich Ilt-Sme relative to fine clays from the Vistula loads (samples V1–V16) and delta-front sediments (samples N1, N2, N3, E2, and E4; Figs 2–4, 8). Additionally, the fine clay fraction of sediments, deposited on the boundary of fresh and brackish waters (V16), showed neither an increase in the amount of illite, kaolinite and/or chlorite nor a decrease in the amount of smectite-rich Ilt-Sme, relative to fresh-water sediments. These facts indicated that although detrital flux is the most important factor, explaining the clay mineral composition in the Gdańsk Bay sediments, the depositional segregation of minerals in the fine clay fraction was not prominent in the environment studied.

The relative abundance of kaolinite in the clay fractions studied showed a uniform distribution of the mineral in

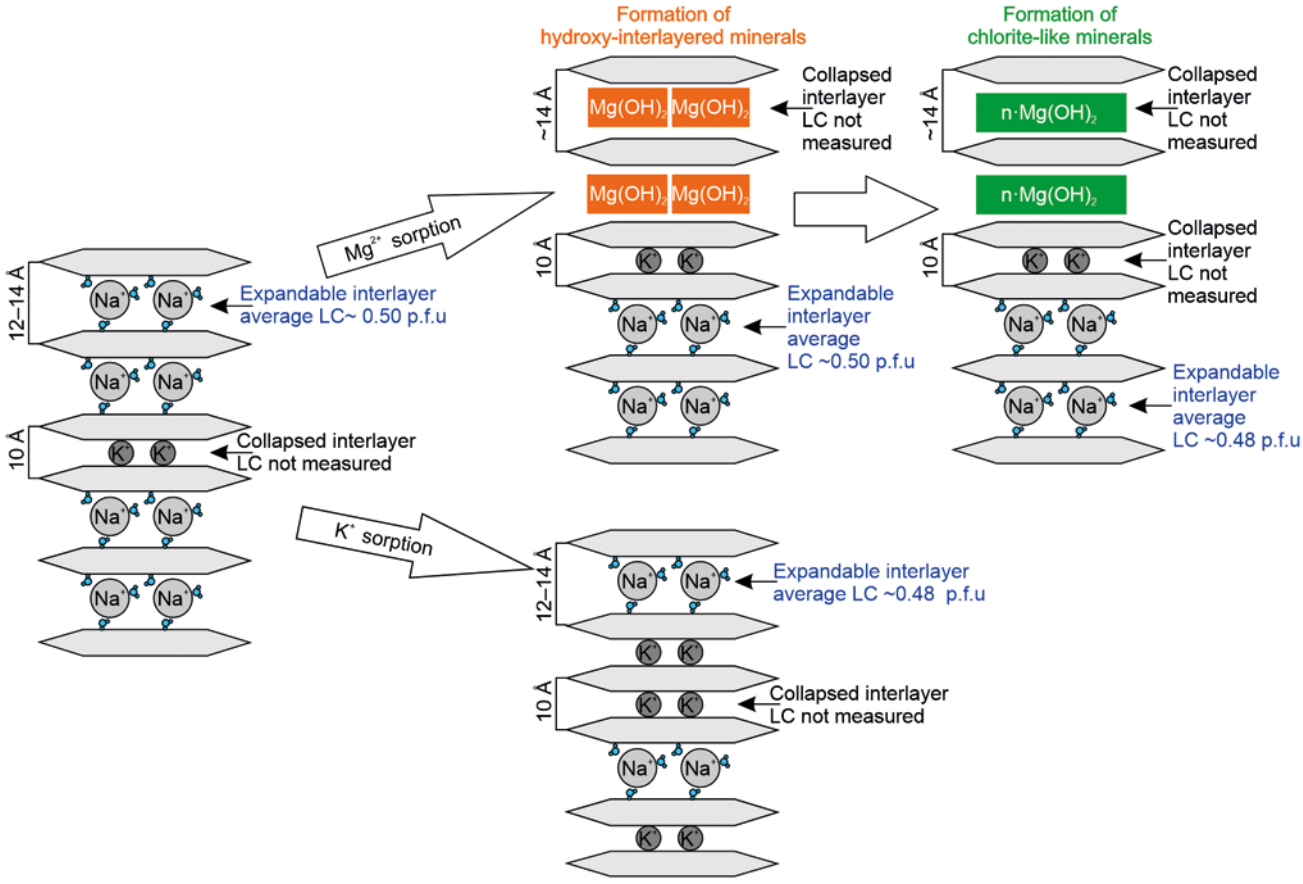

Fig. 11. Summary of the presented results.

the Gdańsk Bay sediments. In general, the formation of kaolinite requires acidic conditions (Wilson, 1999). The neutral pH conditions in the delta-front sediments were not suitable for kaolinite to form. The proper conditions for kaolinization occurred in a few layers of the prodelta sediments, especially in the NE6 core, where the pH obtained was less than 6 (Tab. 2). However, the XRD patterns of oriented specimens of samples having low pH did not show any significant increase in intensities of kaolinite reflections, relative to samples having neutral or slightly alkaline pH. Therefore, there is no evidence of the neoformation of kaolinite. The detrital flux can account for the abundance of kaolinite in the Gdańsk Bay sediments.

The fine clay fraction of prodelta sediments was significantly enriched in K_2O, MgO, and Fe_2O_3 compared to fine clays carried by the Vistula River. Ilt-Sme was the only swelling clay mineral among the fine clay fraction present in the sediments of the Gdańsk Bay. Therefore, it can be concluded that smectitic part of Ilt-Sme was responsible for the uptake of K, Mg, and Fe from the water of Gdańsk Bay. The exchange of ions between swelling clays and the surrounding environment and the transformation of detrital clays most likely led to an immobilization of potassium, magnesium, and iron in the structure of the clay minerals. This type of reverse weathering is observed worldwide (Mackenzie and Garrels, 1966; Mackenzie and Kump, 1995; Michalopoulos and Aller, 1995; Hover *et al.*, 2002; Cuadros *et al.*, 2017).

The presence of di, trioctahedral chlorite in the <2μm fraction and the suspended material of the Vistula loads from the upper, middle, and lower parts of the basin indicated that at least a part of the chlorite in the <2 μm fraction separated from the Gdańsk Bay sediments also was probably of detrital origin. It is worth noting that traces of chlorite probably were present also in those <2 μm fractions, which did not show the mineral presence in the XRD patterns, as indicated by the fact that small amount of chlorite was present in the magnetic subfraction of E4 sample (Fig. 8B). One might argue that a detrital origin accounted for all the chlorite in both clay fractions and it could have been deposited during colder climate periods, when it was able to survive weathering in the alimentation area. The chlorite also could have been supplied, owing to more intense erosion reaching the lower soil horizons. However, over the last 2,500 years, the Vistula basin was relatively stable in terms of landscape transformations and climatic conditions (Mojski, 2005). According to Wanner *et al.* (2008) and Notebaert and Verstraeten (2010), during the Late Holocene, the temperature aberration in Europe did not exceed 3°C relative to the present temperature. Modification of the weathering processes in the alimentation area would require more drastic climate changes (Schroeder, 2016). The surface cover within the catchment was the element of the environment, which changed drastically during that time as a result of human activity – from pristine temperate broadleaf and mixed forests to an almost completely agricultural landscape. The transformation of the landscape most likely intensified the

erosion in the area, owing to deforestation and exposure of the soils. The most intense development of agriculture in the area took place in the 14th and 15th centuries (Brown and Pluskowski, 2011; Czerwiński *et al.*, 2021). Taking into consideration the fact that the oldest core sample was deposited most likely between 407 and 235 BC, if erosion intensity was a significant factor controlling the chlorite supply to Gdańsk Bay, an increased chlorite content would be observed in the middle of the cores studied. However, no fluctuations in chlorite content were observed (Fig. 4). Although chlorite was present in some samples along the entire course of the Vistula, it was most abundant in the coarse fraction of samples from the upper part of the catchment. Most likely, it was due to washing chlorite out of the soils, in which chlorite had been inherited from the bedrock (i.e., soils developed on the igneous rock of the Tatra Mountains or the flysch bedrock of the Outer Carpathian Mountains). The downstream presence of chlorite was rare. In spite of that, it was a substantial component of the fine clay fraction of the prodelta sediments. All these facts indicate the early diagenetic origin of chlorite within fine clay fraction of the prodelta sediments.

The formation of chlorite was probably initiated by the hydroxy-interlayering of smectite, when detrital sediments were deposited near the river mouth. This was indicated by the fact that all the samples from near the river mouth contained HIMs and were slightly depleted in smectite, relative to the Vistula River clays. The prodelta fine clays were even more depleted in smectite, but HIMs were not observed, although the presence of chlorite was noted (Fig. 3). The metal component of the hydroxy-interlayers structure was not recognized; however, di, trioctahedral nature of the chlorite, which was observed at both XRD and ATR-IR spectra (Figs 7, 9), probably indicated the formation of Mg hydroxy-interlayers. Lindgreen *et al.* (2002), studying Maastrichtian sediments, observed that, even though buried, the sediments were only slightly changed diagenetically. As in the Gdańsk Bay sediments, Lindgreen *et al.* (2002) reported Ilt-Sme transformation into chlorite by fixation of brucite interlayers within smectite; however, HIMs were not observed. Presumably, this was due to the more advanced diagenetic reactions that influenced the Maastrichtian sediments, relative to the Gdańsk Bay Holocene sediments, which might have transformed HIMs into chlorite. HIMs, as a precursor of early diagenetic chlorite, was previously suggested by Rich (1968) and Carstea *et al.* (1970). The process of hydroxy interlayering of smectite in the Gdańsk Bay sediments probably proceeded via the replacement of exchangeable cations by hydroxy interlayers within interlayer spaces of the detrital, dioctahedral smectite compound of Ilt-Sme. The most likely chloritization mechanism would be further development of the hydroxy interlayers into continuous octahedral sheets.

Enrichment of the prodelta fine clays in K_2O (Fig. 10), depletion of those sediments in smectite, and slight enrichment in illite relative to the delta-front and Vistula fine clays indicated the uptake of the potassium by smectite layers. Increase in K_2O concentration, even by 1.26% in the prodelta fine clay fraction relative to the river fine clay fraction, is a statistically significant value and corresponds well with the 1% enrichment in K_2O of smectite in the brackish *vs* freshwater sediments of the Mississippi delta plain, reported by Hover *et al.* (2002). Except for potassium uptake, illite can also be formed from kaolinite in the presence of dissolved Fe^{2+} and colloidal Fe^{3+}. Such a reaction is taking place in mangrove forests in a tropical climate, where Fe oxides, abundant in the soils, enter into marine sites, causing destabilization of kaolinite and transformation to Fe-rich illite (Cuadros *et al.*, 2017; Andrade *et al.*, 2018). However, as claimed by those authors, the Fe-rich illite also should be formed from smectite in the delta environments of a temperate climate, because the reaction requires the same K concentration and less Fe than reaction of transformation of kaolinite to Fe-rich illite. In the case studied, the only indirect evidence that could indicate the formation of Fe-rich illite layers is shown in the XRD patterns of the magnetic subfraction (Fig. 8). The relative intensities of Ilt-Sme and illite reflections changed in both of the Gdańsk Bay environments studied. The amount of Ilt-Sme decreased, while the illite increased, when compared with the magnetic subfraction of the Vistula loads. However, one cannot exclude the possibility that incomplete separation of magnetic and non-magnetic subfractions was responsible for the abundance of those minerals in the magnetic subfraction. Given these uncertainties, Fe-illite formation cannot be treated as a significant reaction, taking place in the study area.

On the other hand, K fixation is well established, not only by ICP-OES analysis, but also is in agreement with the LC measurements by the O-D method. The layer charges of prodelta fine clays were lower and more uniform, relative to fine clays, separated from the Vistula and delta-front sediments (Tab. 2). The decrease may be explained under the assumption that before reaching Gdańsk Bay, there was LC heterogeneity among expandable components of the detrital clays (i.e., more vermiculitic and more smectitic LCs were present). The high-charge constituents most likely selectively adsorbed and fixed K^+ from brackish waters of bay, while the layers with a smectite-like charge remained occupied by hydrated cations (Fig. 11). In other words, the adsorption of potassium ions by the high-charge layers caused the collapse of the interlayer spaces, making them unavailable for D_2O exchange. As a result, the apparent LC, measured by the O-D method, decreased.

Calculating even a rough ratio between high- and low-charge swelling phases in the samples studied was impossible. However, it is worth noting that regardless of the abundance of high-charge clays – since the adsorption stopped, when the LC dropped to ~0.48 p.f.u. – it is reasonable to assume that the layers with average charges >0.48 p.f.u. in early diagenetic conditions are characterized by higher affinities to K^+ than the layers with lower charges. The range of the layer charges obtained is remarkably uniform and close to the values obtained by Kuligiewicz *et al.* (2018), who reported that smectitic components of Ilt-Sme had a constant LC (0.47 ± 0.3 p.f.u.), regardless of the degree of illitization taking place in burial diagenesis.

Selective potassium adsorption by high-charge swelling clays, which was observed in laboratory experiments as well as in studies in the natural environment, resulted in the fixation of K^+ within interlayer space and contraction of the

clay structure to 10 Å (Powers, 1957a, b; Hover *et al.*, 2002; Skiba, 2013). Such K-rich smectite is indistinguishable from true illite on XRD patterns. Therefore, because the minerals were identified here on the basis of XRD, the K-rich smectite that collapsed to 10 Å was called illite. Taking into consideration the results of the O-D method and the mineral and chemical composition of clay fraction that underwent early diagenetic reactions, one may conclude that during reverse weathering the smectite most likely underwent an ion-exchange reaction, not a true illitization. However, more detailed studies (on an atomic scale) of the products of such reactions would be required to observe the reorganization of elements, not only in interlayer spaces, but also in tetrahedral and octahedral sheets.

The early diagenetic formation of chlorite and illite-like minerals in the environment studied is in good agreement with suggestions previously made about that environment by Stoch *et al.* (1980) and with the data and interpretations of the clay mineralogy of deltas and estuaries by Grim (1953), Powers (1953, 1957a, b), Nelson (1958, 1962), Rich (1968), Hover *et al.* (2002). Such early diagenetic transformation of soil-derived swelling clays also is consistent with the results of experimental studies into the long-term interaction of the clays with seawaters, performed by Whitehouse and McCarter (1956), Carroll and Starkey (1958), and Skiba (2013).

CONCLUSIONS

The clay fraction carried in the Vistula River loads is dominated by Ilt-Sme. As shown by the O-D analyses, the expandable component of the Ilt-Sme is characterized by a high charge. When considering the origin of clay minerals in the sediments of Gdańsk Bay, detrital input undoubtedly plays a major role. Nevertheless, early diagenetic transformation also has to be taken into account. The high-charge smectitic component of Ilt-Sme deposited by the Vistula River in Gdańsk Bay was not stable and underwent chloritization and illitization. The chloritization proceeded most likely via transformation of the detrital smectitic component of Ilt-Sme into hydroxy-interlayer minerals. The further development of the hydroxy interlayers most likely produced continuous octahedral sheets within chlorite interlayer space. On the other hand, selective adsorption and dehydration, leading to fixation of K^+ by high-charge expandable interlayers (i.e., smectitic and likely vermiculitic layers), was the most likely mechanism for the early diagenetic formation of an illite-like phase (Fig. 11). The data presented indicate that K, Mg, and Fe cations are being taken up from the overlying and/or interstitial water and stored within the sediments even in a brackish environment. Moreover, no neoformation is required for a cation sink. Therefore, the high-charge smectitic component of Ilt-Sme, derived from soils of humid temperate or continental climate, constitutes abundant reactants that play an especially important part among minerals in element cycling. Furthermore, experimental studies of the reaction of the separated clay fraction with various types of seawater might give additional insight into the exchange of cations between clays and water and clay mineral transformation, which might be useful in the modeling of diagenetic processes in sedimentary basins.

Acknowledgements

This manuscript and the research behind it would not have been possible without the invaluable support of many people, from friends and family helping with fieldwork to J. M. Wampler, whose insightful comments greatly improved the manuscript. We would also like to acknowledge effort of two anonymous reviewers and editors: Bartosz Budzyń, Ewa Malata, and Frank Simpson for proofreading of the texts and theirs numerous, helpful recommendations. We express deep gratitude to each and every one. This work was financed by the Polish National Science Centre [Grant Number 2016/23/N/ST10/01388].

REFERENCES

Andrade, G. R. P., Cuadros, J., Partiti, C. S. M., Cohen, R. & Vidal-Torrado, P., 2018. Sequential mineral transformation from kaolinite to Fe-illite in two Brazilian mangrove soils. *Geoderma*, 309: 84–99.

Baldermann, A., Warr, L. N., Grathoff, G. H. & Dietzel, M., 2013. The rate and mechanism of deep-sea glauconite formation at the Ivory Coast-Ghana Marginal Ridge. *Clays and Clay Minerals*, 61: 258–276.

Barnhisel, R. I. & Bertsch, P. M., 1989. Chlorites and hydroxy-interlayered vermiculite and smectite. In: Dixon, J. & Weed, S. (eds), *Minerals in Soil Environments*. *2nd ed*. Soils Science Society of America, Madison, pp. 729–788.

Brown, A. & Pluskowski, A., 2011. Detecting the environmental impact of the Baltic Crusades on a late-medieval (13th–15th century) frontier landscape: Palynological analysis from Malbork Castle and hinterland, Northern Poland. *Journal of Archaeological Science*, 38: 1957–1966.

Burst, J. F., 1958. Glauconite pellets: their mineral nature and applications to stratigraphic interpretations. *AAPG Bulletin*, 42: 310–327.

Carroll, D. & Starkey, H., 1958. Effect of sea-water on clay minerals. *Clays and Clay Minerals*, 7: 80–101.

Carstea, D. D., Harward, M. E. & Knox, E. G., 1970. Formation and stability of hydroxy-Mg interlayers in phyllosilicates. *Clays and Clay Minerals*, 18: 213–222.

Chamley, H., 1989. Estuaries and deltas. In: Chamley, H. (ed.), *Clay Sedimentology*. Springer, Berlin, Heidelberg, pp. 97–116.

Christidis, G. E. & Eberl, D. D., 2003. Determination of layer-charge characteristics of smectites. *Clays and Clay Minerals*, 51: 644–655.

Cuadros, J., Andrade, G., Ferreira, T. O., de Moya Partiti, C. S., Cohen, R. & Vidal-Torrado, P., 2017. The mangrove reactor: Fast clay transformation and potassium sink. *Applied Clay Science*, 140: 50–58.

Cyberska, B., 1990. Zasolenie wód Basenu Gdańskiego. In: Majewski, A. (ed.), *Zatoka Gdańska*. Wydawnictwa Geologiczne, Warszawa, pp. 237–255. [In Polish.]

Czerwiński, S., Guzowski, P., Lamentowicz, M., Gałka, M., Karpińska-Kołaczek, M., Poniat, R., Łokas, E., Diaconu, A. C., Schwarzer J., Miecznik, M. & Kołaczek, P., 2021. Environmental implications of past socioeconomic events in

Greater Poland during the last 1200 years. Synthesis of paleoecological and historical data. *Quaternary Science Reviews*, 259: 106902.

Damrat, M., Zaborska, A. & Zajaczkowski, M., 2013. Sedimentation from suspension and sediment accumulation rate in the River Vistula prodelta, Gulf of Gdańsk (Baltic Sea). *Oceanologia*, 55: 937–950.

Dietel, J., Gröger-Trampe, J., Bertmer, M., Kaufhold, S., Ufer, K. & Dohrmann, R., 2019. Crystal structure model development for soil clay minerals – I. Hydroxy-interlayered smectite (HIS) synthesized from bentonite. A multi-analytical study. *Geoderma*, 347: 135–149.

Dunn, O. J., 1964. Multiple comparisons using rank sums. *Technometrics*, 6: 241–252.

Eberl, D. D., 1984. Clay mineral formation and transformation in rocks and soil. *Philosophical Transactions of the Royal Society of London*, 311: 241–257.

Emelyanov, E. M. & Stryuk, V., 2002. Distribution of suspended matter. In: Emelyanov, E. M. (ed.), *Geology of the Gdańsk Basin, Baltic Sea*. Yantarny Skaz. Russian Academy of Sciences - P. P. Shirshov Institute of Oceanology, Kaliningrad, pp. 78–81.

Górnik, M., 2018. Long-term (1951–2015) changes in runoff along Poland's rivers Vistula and Bug. *Przegląd Geograficzny*, 90: 479–494.

Griffin, J. J., Windom, H. & Goldberg, E. D., 1968. The distribution of clay minerals in the World Ocean. *Deep Sea Research and Oceanographic Abstracts*, 15: 433–459.

Grim, R. E., 1953. Clay mineral investigation of sediments in the northern Gulf of Mexico. *Clays and Clay Minerals*, 2: 81–103.

Hover, V. C., Walter, L. M. & Peacor, D. R., 2002. K uptake by modern estuarine sediments during early marine diagenesis, Mississippi Delta Plain, Louisiana, U.S.A. *Journal of Sedimentary Research*, 72: 775–792.

Institute of Meteorology and Water Management – National Research Institute, 2022. https://klimat.imgw.pl/pl/climate-normals/ [In Polish, 2-Dec-2022.]

Isson, T. T. & Planavsky, N. J., 2018. Reverse weathering as a long-term stabilizer of marine pH and planetary climate. *Nature*, 560(7719): 471–475.

Isson, T. T., Planavsky, N. J., Coogan, L. A., Stewart, E. M., Ague, J. J., Bolton, E. W., Zhang, S., McKenzie, N. R.& Kump, L. R., 2020. Evolution of the global carbon cycle and climate regulation on earth. *Global Biogeochemical Cycles*, 34: e2018GB006061.

Jackson, M. L., 1969. *Soil Chemical Analysis: Advanced Course. 2nd Ed*. Madison, Wisconsin, 895 pp.

Kottek, M., Grieser, J., Beck, C., Rudolf, B. & Rubel, F., 2006. World Map of the Köppen-Geiger climate classification updated. *Meteorologische Zeitschrift*, 15: 259–263.

Kruskal, W. H. & Wallis, W. A., 1952. Use of ranks in One-Criterion Variance Analysis. *Journal of the American Statistical Association*, 47(260): 583–621.

Kuligiewicz, A., Derkowski, A., Emmerich, K., Christidis, G. E., Tsiantos, C., Gionis, V. & Chryssikos, G. D., 2015a. Measuring the layer charge of dioctahedral smectite by O-D vibrational spectroscopy. *Clays and Clay Minerals*, 63: 443–456.

Kuligiewicz, A., Derkowski, A., Szczerba, M., Gionis, V. & Chryssikos, G. D., 2015b. Revisiting the infrared spectrum of the water-smectite interface. *Clays and Clay Minerals*, 63: 15–29.

Kuligiewicz, A., Derkowski, A., Środoń, J., Gionis, V. & Chryssikos, G. D., 2018. The charge of wettable illite-smectite surfaces measured with the O-D method. *Applied Clay Science*, 161: 354–363.

Lanson, B., Ferrage, E., Hubert, F., Prêt, D., Mareschal, L., Turpault, M. P. & Ranger, J., 2015. Experimental aluminization of vermiculite interlayers: An X-ray diffraction perspective on crystal chemistry and structural mechanisms. *Geoderma*, 249–250: 28–39.

Lindgreen, H., Drits, V. A., Sakharov, B. A., Jakobsen, H. J., Salyn, A. L., Dainyak, L. G. & Krøyer, H., 2002. The structure and diagenetic transformation of illite-smectite and chlorite-smectite from North Sea Cretaceous-Tertiary chalk. *Clay Minerals*, 37: 429–450.

Mackenzie, F. T. & Garrels, R. M., 1966. Chemical mass balance between rivers and oceans. *American Journal of Science*, 264: 507–525.

Mackenzie, F. T. & Kump, L. R., 1995. Reverse weathering, clay mineral formation, and oceanic element cycles. *Science*, 270: 586–587.

Majewski, W., 2013. General characteristics of the Vistula and its basin. *Acta Energetica*, 2: 6–15.

Mehra, O. P. & Jackson, M. L., 1958. Iron oxide removal from soils and clays by a dithionite-citrate system buffered with sodium bicarbonate. *Clays and Clay Minerals*, 7: 317–327.

Meunier, A., 2007. Soil hydroxy-interlayered minerals: A reinterpretation of their crystallochemical properties. *Clays and Clay Minerals*, 55: 380–388.

Michalopoulos, P. & Aller, R. C., 1995. Rapid clay mineral formation in Amazon delta sediments: Reverse weathering and oceanic elemental cycles. *Science*, 270(5236): 614–617.

Mojski, E., 2005. *Ziemie polskie w czwartorzędzie. Zarys morfogenetyczny*. Polish Geological Institute – National Research Institute, Warszawa, 404 pp. [In Polish.]

Moore, D. M. & Reynolds, R. C., Jr., 1997. *X-Ray Diffraction and the Identification and Analysis of Clay Minerals. 2nd ed*. Oxford University Press, New York, 400 pp.

Nelson, B. W., 1958. Clay Mineralogy of the Bottom Sediments, Rappahannock River, Virginia. *Clays and Clay Minerals*, 7: 135–147.

Nelson, B. W., 1962. Clay mineral diagenesis in the Rappahannock estuary: an explanation. *Clays and Clay Minerals*, 11: 210–210.

Notebaert, B. & Verstraeten, G., 2010. Sensitivity of West and Central European river systems to environmental changes during the Holocene: A review. *Earth-Sci Reviews*, 103: 163–182.

Odin, G. S. & Fullagar, P. D., 1988. Geological significance of the glaucony facies. In: Odin, G. S. (ed.), *Developments in Sedimentology.* Elsevier, Amsterdam, pp. 295–332.

Powers, M. C., 1953. Clay diagenesis in the Chesapeake Bay area. *Clays and Clay Minerals*, 2: 68–80.

Powers, M., 1957a. Adjustment of land derived clays to the marine environment. *SEPM Journal of Sedimentary Research,* 27: 355–372.

Powers, M. C., 1957b. Adjustment of clays to chemical change and the concept of the equivalence level. *Clays and Clay Minerals*, 6: 309–326.

Pugliese Andrade, G. R., de Azevedo, A. C., Cuadros, J., Souza, V. S., Correia Furquim, S. A., Kiyohara, P. K. & Vidal-Torrado, P., 2014. Transformation of kaolinite into smectite and iron-illite in Brazilian mangrove soils. *Soil Science Society of America Journal*, 78: 655–672.

Rich, C. I., 1968. Hydroxy interlayers in expansible layer silicates. *Clays and Clay Minerals*, 16: 15–30.

Russell, J. & Fraser, A., 1994. Infrared methods. In: Wilson, M. (ed.), *Spectroscopic and Chemical Determinative Methods. Clay Mineralogy*. Chapman and Hall, London, pp. 11–67.

Schroeder, P., 2002. Infrared spectroscopy in clay science. *Teaching Clay Science*, 11: 181–206.

Schroeder, P., 2016. *Clays in the Critical Zone: An Introduction*. Cambridge University Press, United Kingdom, Cambridge, 246 pp.

Skiba, M., 2013. Evolution of dioctahedral vermiculite in geological environments – an experimental approach. *Clays and Clay Minerals*, 61: 290–302.

Skiba, M., Skiba, S., Derkowski, A., Maj-Szeliga, K. & Dziubińska, B., 2018. Formation of NH_4-illite-like phase at the expense of dioctahedral vermiculite in soil and diagenetic environments – an experimental approach. *Clays and Clay Minerals*, 66: 75–85.

Środoń, J., 2006. Identification and quantitative analysis of clay minerals. In: Bergaya, F., Theng, B. K. G. & Lagaly, G. (eds), *Handbook of Clay Science*. *2nd ed*. *Developments in Clay Sciences, Vol. 1.* Elsevier, Amsterdam, pp. 765–787.

Stoch, L., Görlich, K. & Pieczka, F. B., 1980. Litologia i skład mineralny osadów z dna Basenu Gdańskiego. *Kwartalnik Geologiczny*, 24: 395–414. [In Polish, with English summary.]

Tellier, K. E., Hluchy, M. M., Walker, J. R. & Reynolds, R. C., 1988. Application of high gradient magnetic separation (HGMS) to structural and compositional studies of clay mineral mixtures. *Journal of Sedimentary Research*, 58: 761–763.

Uścinowicz, S. & Zachowicz, J., 1993a. *Geological Map of the Baltic Sea Bottom, Gdańsk Deep sheet. Scale 1: 200 000*. Polish Geological Institute – National Research Institute, Warsaw.

Uścinowicz, S. & Zachowicz, J., 1993b. *Geological Map of the Baltic Sea Bottom, Elbląg sheet. Scale 1: 200 000*. Polish Geological Institute – National Research Institute, Warsaw.

Uścinowicz, S. & Zachowicz, J., 1993c. *Geological Map of the Baltic Sea Bottom, Gdańsk sheet. Scale 1: 200 000*. Polish Geological Institute – National Research Institute, Warsaw.

Uścinowicz, S., Ebbing, J., Laban, C. & Zachowicz, J., 1998. Recent muds of the Gulf of Gdańsk. *Baltica*, 11: 25–32.

Velde, B. & Church, T., 1999. Rapid clay transformations in Delaware salt marshes. *Applied Geochemistry*, 14: 559–568.

Wanner, H., Beer, J., Bütikofer, J., Crowley, T. J., Cubasch, U., Flückiger, J., Goosse, H., Grosjean, M., Joos, F., Kaplan, J. O., Küttel, M., Müller, S. A., Prentice, I. C., Solomina, O., Stocker, T. F., Tarasov, P., Wagner, M. & Widmann, M., 2008. Mid- to Late Holocene climate change: an overview. *Quaternary Science Reviews*, 27: 1791–828.

Weaver, C. E., 1989. *Clays, Muds, and Shales*. Elsevier, Amsterdam, 820 pp.

Whitehouse, U. G. & McCarter, R. S., 1956. Diagenetic modification of clay mineral types in artificial sea water. *Clays and Clay Minerals*, 5: 81–119.

Wiewióra, A., Giresse, P., Petit, S. & Wilamowski, A., 2001. A deep-water glauconitization process on the Ivory Coast-Ghana Marginal Ridge (ODP Site 959): Determination of Fe^{3+}-rich montmorillonite in green grains. *Clays and Clay Minerals*, 49: 540–558.

Wilson, M. J., 1999. The origin and formation of clay minerals in soils: past, present and future perspectives. *Clay Minerals*, 34: 7–25.